EFFECT OF ACTUATION PARAMETERS ON STABILIZATION OF METHANE DIFFUSIVE FLAMES USING PLASMA ACTUATORS

M.G. De Giorgi*, A. Ficarella*, A. Sciolti*, S. Campilongo*, E. Pescini*, G. di Lecce**

mariagrazia.degiorgi@unisalento.it
*University of Salento, Dipartimento di Ingegneria dell'Innovazione, Lecce, Italy
**NANOTEC, Istituto di Nanotecnologie (CNR) - UOS Bari - Italy

Abstract
The reduction of nitric oxides (NOx) in aircraft engines, gas turbines, or internal combustion engines is a main issue in the design of novel combustion systems. The reduction of the NOx emissions might be reached by lean combustion. However, the major issue is the stabilization of the flame under lean conditions.
In this context, the present work investigates the possibility of increasing the combustion efficiency of a lean flame through the employment of a plasma actuator, operated by both nanosecond repetitively pulsed high voltage (NRPP) and sinusoidal DBD high voltage (HV). Different actuation conditions have been tested to stabilize and improve the efficiency of a lean non premixed methane/air flame in a Bunsen-type coaxial burner with central fuel jet. An image processing approach was used to characterize the flame behavior near blowout conditions.

Introduction
The reduction of pollutant emissions has become a major issue in the development of combustion engines systems. Nitric oxides (NOx) emissions are strongly related to the flame temperature [1], which is influenced by the fuel equivalence ratio. The temperature can be reduced by burning the fuel in lean conditions [2]. However, in these conditions, the flame shows instabilities and eventually extinction events [3]. Lean blowout (LBO) is a major technical challenge for low emission combustion systems. In the past previous studies showed that an electric field can positively affect the flame stability, the flame propagation speed, and the combustion chemistry, also at lean conditions [4].
However, the precise mechanism by which combustion is enhanced by electrical plasma discharges is still not well understood.
Several studies focused on the application of high-voltage pulses to improve the ignition of fuel/air mixtures [5, 6]. In [7] and [8] it was shown that nanosecond high-voltage pulses might reduce the ignition delay time. Few works were focused on the application of the plasma actuation for the flame stabilization [9, 10] [].
A plasma actuator is substantially a device able to change locally the chemical and fluid dynamic state using the action of an applied electric field [11].
In [12] Nanosecond Repetitively Pulsed (NRP) discharges produced by electric

pulses of about 10 kV during 10 ns, and at a frequency of 30 kHz, where applied to stabilize a lean premixed methane/air flame at atmospheric pressure.

It was shown that the plasma created in the recirculation zone permits to stabilize the lean flame and to reduce the lean extinction limit by about 10-15%, with a plasma power that was less than 1% of the power of the flame. In [13] a repetitive discharge at 9 kHz, with voltage pulse duration of order 100ms was used to extend the flammability limit of a lean propane/air mixture at atmospheric pressure.

Previous studies investigated the plasma actuation mainly in premixed burners or coaxial burner with central fuel jet. However, in several fields reverse configurations with central oxidizer jet surrounded by annular fuel jet are of great interest. Because of the varied applications of this last configuration ranging from rocket combustor to gas burners, there is need of stabilizing the flame in conditions near the blowout [14]. In the present work, both sinusoidal and nanosecond repetitively pulsed plasma actuation, have been used to stabilize and improve the efficiency of a lean non premixed methane/air flame in a non-premixed Bunsen-type burner with annular fuel jet.

Experimental set-up

The plasma generation
The experiments were realized using a specifically designed burner equipped with a plasma actuator, as sketched in Fig.1 (a). A coaxial cylindrical DBD configuration has been used. The outer electrode (hereafter noted as "HV electrode") is a 3 cm long stainless steel mesh that surrounds a quartz tube (with an inner diameter of 10 mm and a thickness of 1 mm), and it is connected to a HV generator. The inner electrode (hereafter noted as "grounded electrode") is a hollow stainless steel tube having an outer diameter of 8 mm and an inner diameter of 6 mm. The region between the top end of the steel tube and the top end of the quartz tube (mixing region) is 40 mm and the standoff distance (distance between the end of the HV electrode and the end of the internal steel tube) is 6 mm.

The electrical system was composed by a dedicated personal computer (PC), a high voltage (HV) amplifier that supplied the actuator, a high voltage probe (Tektronix P6015A [15]), a current probe (Bergoz Current Transformer CT-C1.0-B [16]) and an oscilloscope (Tektronix TDS2024C [17]). The HV probe was located on the HV connector side and the current probe on the ground side. A Faraday gage has been used to shield the cameras from any electromagnetic interference due to the high electric fields required to generate the plasma discharge. Two different HV generators were used. The first one is a nanosecond pulse generator (NPG-18/3500 of MegaImpulse Ltd® [18]), which produces high voltage pulses characterized by: a maximum peak voltage of 40 kV, a pulse rise time of about 4 ns, a pulse repetition rate up to 3.5 kHz and an energy up to 30mJ/pulse. The second one is the Dielectric Barrier Corona and Plasma Discharge Resonant Driver commercialized by Information Unlimited® [19]. It leads instead to a sinusoidal waveform

actuation signal with different voltage amplitudes up to 8 kV and frequency of 20 kHz. Both the high voltage probe and the current transformer were connected to an oscilloscope, and the respective signals were recorded with an accuracy of $\pm 3\%$. The acquired data allowed retrieving the discharge-current characteristic curves in function of the actuation time (t), useful for evaluating the electrical power dissipation. In a single acquisition the oscilloscope recorded 2500 points at a sampling rate of 25 MHz, therefore two periods (T) for each waveform. For each input voltage, 128 acquisitions were recorded and averaged. An example of an averaged acquisition is reported in Fig.1 (b).

The averaged voltage $\overline{V}(t)$ and current $\overline{I}(t)$ data were after used for electric power dissipation $\overline{P}_{el}$, calculated by:

$$\overline{P}_{el} = \frac{1}{2T} \int_{0}^{2T} \overline{I}(t)\overline{V}(t)dt \qquad (1)$$

Numerical integration was performed by the trapezoidal rule and the corresponding uncertainty, estimated by standard uncertainty analysis methodology [20], resulted in $\pm 4\%$.

Figure 1 (c) reports the power dissipation in function of the operating voltage in the case of the sinusoidal voltage waveform, expressed as a percentage of the HV amplifier maximum output. To test the capability of the nanosecond pulse to control the flame, different levels of voltage and pulse repetition rate were applied. Both the voltage and the frequency were set to 0% (hereafter noted as "NO PLASMA condition"), 25%, 50%, 75%, 100%, which correspond to 0, 10, 20, 30, 40 kV and 0, 875, 1750, 2625, 3500 Hz. The plasma actuation acted on the fuel, which was fueled in the outer coaxial tube (the air was instead fueled in the inner tube). The study of the influence of the plasma on flame blowout limits (LBO) was performed by holding the methane flow rate constant at a certain value and increasing the air-flow rate until firstly the flame flashback occurred and then the flame blew out. This procedure was repeated for different values of methane flow rate and air flow rate, in correspondence of which blowout occurred and the respective flow rates were recorded. The flow rates of air and methane are controlled by two flow meters: the SFAB-50U-HQ12-2SV-M12 of Festo® [21] for the air and the BGR of Baggi® [22] for the methane. All the experiments were conducted keeping the pressure at 1.01325 bar and the gas inlet temperature (for both fuel and air) at 288 K.

The visible flame appearance was captured using a Canon Power Shot SX240 HS digital camera with the following settings: ISO 800, focal length of 18 mm, aperture of f/8.0 and an exposure time of 1/8 s. The high speed events, occurring towards blowout, were captured using the high speed CCD camera MEMRECAM GX-3® of NAC Image Technology (visible spectral range emission) [23], which was used with a frame rate of 200 Hz. The broadband chemiluminescence was

acquired using a CCD by La Vision® [24], equipped with an intensifier by Lambert Instrumentation® [25].
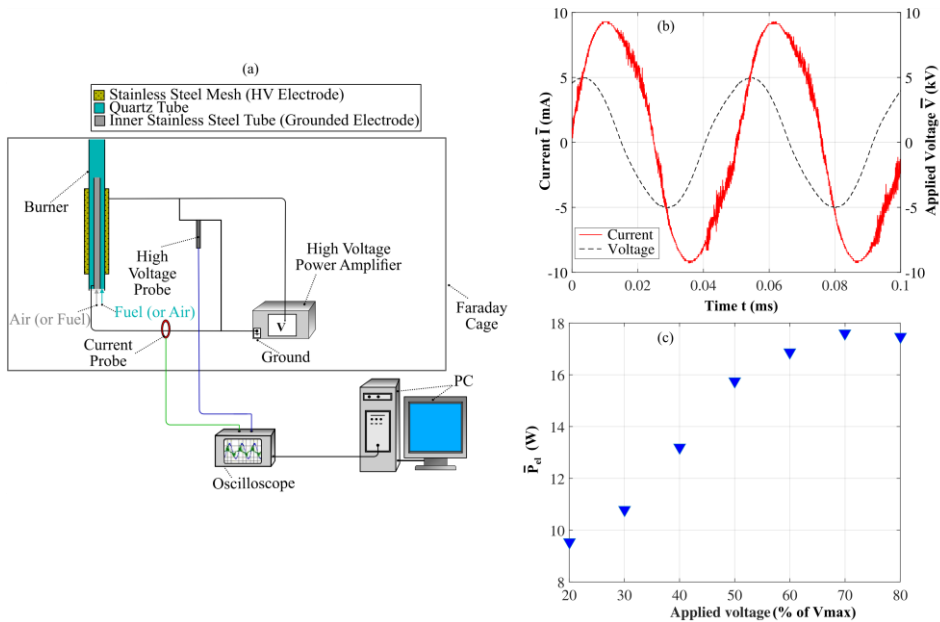

Figure 1. (a) Experimental setup; (b) Current-Voltage characteristic curves at 50% of the HV amplifier maximum output; (c) Power dissipation as function of the applied voltage expressed as a percentage of the HV amplifier maximum output
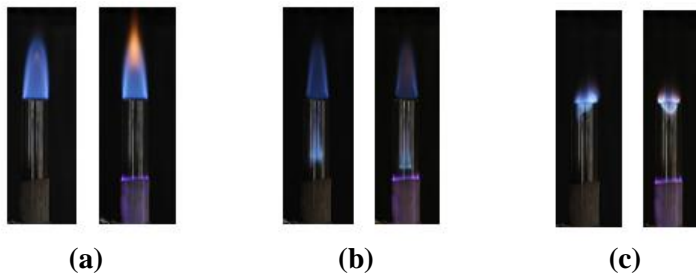

| (a) | (b) | (c) |

Figure 2. Flame images at fuel flow rate 0.465 l/min and different air flow rates: (a) 7.5 l/min, (b) 4 l/min, (c) 2.5 l/min. For each condition, on the left: NO PLASMA condition; on the right: sinusoidal HV (20 % V_{max}, 20 kHz).

Results

Figure 2 shows the flame image acquired from rich to lean flame conditions without and with plasma actuation. In particular, the sinusoidal voltage actuation is considered. The actuation produces significant change in the flame shape and improves the stability and the homogeneity of the flame.

In particular in rich conditions, which means low air flow rate, the plasma actuation does not produce effects on the flame shape even if it leads to an increase of the flame intensity. Towards lean conditions it is evident the enhanced anchoring of the flame on the edge of the quartz tube. In this condition the effect of actuation is mainly related to the stabilization of the flame and the rise of the blowout limit. Figure 3 shows that a high rise in the amplitude voltage leads to an evident improvement of the LBO limit, which is reached at an air flow rate that is approximately three times higher than the NO PLASMA condition.
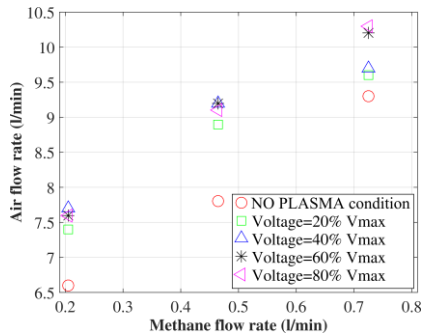

Figure 3. LBO limits for different values of methane flow rate. Actuation with sinusoidal HV at 20 kHz and different voltage amplitudes, expressed as a percentage of the HV amplifier maximum output
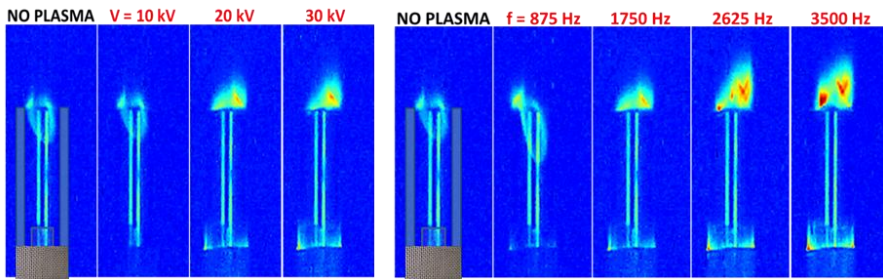

Figure 4. Broadband chemiluminescence: actuation by NRPP (fuel flow rate equal to 0.2 l/min, baseline air flow rate = 5.2 l/min); on the left: different applied voltage at 1750 Hz, on the right: different repetition frequency at 20% of V_{max}

Table 1. Percentage rise of LBO limits for different values of amplitude and repetition frequencies of the NRPP and the sinusoidal voltages (fuel flow rate equal to 0.2 l/min).

	Sinusoidal DBD at 20kHz	NRPP at 1750 Hz	NRPP at 3500 Hz
40 % of V_{max}	16.7 %	6.5%	3.2%
60 % of V_{max}	15.1 %	0%	17.7%
80 % of V_{max}	15.1 %	12.9%	32.3%

Figure 4 shows the broadband chemiluminescence images in the case of actuation by NRPP, to underline the effect of the actuation amplitude voltage and of the repetition frequency. It is evident that the rise of these parameters improves the performance of the NRPP actuation. Table 1 compares the rise of the LBO that has been reached with the different actuation methods at a fixed fuel flow rate. It is evident that the NRPP, at the high voltage and repetition rate, outperforms the other actuation conditions, with a rise up to approximately 32% with respect to the baseline condition with NO PLASMA.

Conclusions

In the present work it was demonstrated the possibility to increase the combustion efficiency of a lean non premixed methane flame through the use of a plasma actuators acting on the fuel flow under different actuation conditions. In particular, sinusoidal voltage DBD and nanosecond repetitively pulsed plasma (NRPP) operating conditions were tested.
The plasma actuation permits an evident increase of the air flow rate that leads to flame blowout for both the actuation methods, even if nanosecond pulsed DBD outperformed the sinusoidal one in terms of rise of the LBO limits. The effect of actuation on the flame shape has been also recorded using visual observations. The enlargement of the stability region permits to use ultra-lean mixtures and to produce fewer pollutants into the atmosphere, while maintaining a stable flame.

Fundings

References
[1] A.H. Lefebvre, D.R. Ballal, Gas turbine combustion, CRC Press, 2010.
[2] G.L. Pilla, D.A. Lacoste, D. Veynante, C.O. Laux, Plasma Science, IEEE Transactions on, 36 (2008) 940-941.
[3] M.G. De Giorgi, A. Sciolti, S. Campilongo, A. Ficarella, in: ASME 2014 Power Conference, American Society of Mechanical Engineers, 2014, pp. V001T001A001-V001T001A001.
[4] L. Rosocha, D. Coates, D. Platts, S. Stange, Physics of Plasmas (1994-present), 11 (2004) 2950-2956.
[5] A. Klimov, V. Byturin, V. Brovkin, V. Vinogradov, D. Van Wie, in: AIAA, Aerospace Sciences Meeting and Exhibit, 39 th, Reno, NV, 2001.
[6] A. Bao, Y.G. Utkin, S. Keshav, G. Lou, I.V. Adamovich, Plasma Science, IEEE Transactions on, 35 (2007) 1628-1638.
[7] N. Anikin, E. Kukaev, S. Starikovskaia, A. Starikovskii, AIAA Paper, 833 (2004) 5-8.

[8] S.M. Starikovskaia, Journal of Physics D: Applied Physics, 39 (2006) 265.

[9] Y. Kim, V.W. Ferreri, L. Rosocha, G.K. Anderson, S. Abbate, K.-T. Kim, Plasma Science, IEEE Transactions on, 34 (2006) 2532-2536.

[10] M. Cha, S. Lee, K. Kim, S. Chung, Combustion and flame, 141 (2005) 438-447.

[11] E. Pescini, M.G. De Giorgi, L. Francioso, A. Sciolti, A. Ficarella, Science, Measurement & Technology, IET, 8 (2014) 135-142.

[12] Q.L.L. Pham, D.A. Lacoste, C.O. Laux, Plasma Science, IEEE Transactions on, 39 (2011) 2264-2265.

[13] W.-S. Choi, Y. Neumeier, J. Jagoda, AIAA paper, 982 (2004) 2004.

[14] S. Mahesh, D.P. Mishra, Combustion and Flame, (2015).

[15] V.V.A.A., Tektronix P6015A specifications URL: http://uk.tek.com/datasheet/high-voltage-probe-single-ended/p5100a-tpp0850-p5122-p5150-p6015a-datasheet-0.

[16] V.V.A.A., Bergoz Current Transformer CT-C1.0-B specifications URL: http://www.gmw.com/electric_current/Bergoz/documents/CT.11flyer.PDF.

[17] V.V.A.A., Tektronix TDS2024C specifications URL: http://www.testequipmentdepot.com/tektronix/oscilloscope/tds2024c.htm.

[18] V.V.A.A., NPG 18-3500 specifications URL: http://megaimpulse.com/info/User_Manual_NPG_18_3500.pdf.

[19] V.V.A.A., Dielectric Barrier Corona and Plasma Discharge Resonant Driver by Information Unlimited® specifications: URL http://www.amazing1.com/products/dielectric-barrier-corona-and-plasma-discharge-resonant-driver.html

[20] R.J. Moffat, Experimental thermal and fluid science, 1 (1988) 3-17.

[21] V.V.A.A., Festo Flowmeter specifications URL: http://www.festo.com/net/fi_fi/SupportPortal/default.aspx?cat=1959&q=SFAB&tab=3&type=92.

[22] V.V.A.A., Baggi flow meters URL: http://www.baggi.com/datafiles/downloads/TDSMZ110520AR0_EN_biogas%20MFM%20flow%20meter.pdf.

[23] V.V.A.A., Memrecam® specifications. URL: http://www.nacinc.com/products/memrecam-high-speed-digital-cameras/gx-3/.

[24] V.V.A.A., La Vision ICCD ICCD at URL: http://www.lavision.de/en/products/cameras/iccd_cameras.php.

[25] V.V.A.A., High-Speed Intensified Camera Attachment specifications URL: http://www.lambertinstruments.com/hicatt.